

CONSTRAINTS ON CRATER GROWTH MECHANISMS, EJECTA THICKNESSES AND EXCAVATION DEPTHS FROM TARGET OUTCROPS AT FRESH LUNAR CRATERS. V. L. Sharpton, Lunar and Planetary Institute, 3600 Bay Area Blvd., Houston TX 77058; sharpston@lpi.usra.edu.

Introduction: The elevated rims of impact craters consist of fragmental ejecta emplaced onto target rock that is structurally uplifted from its pre-impact level during the excavation stage of the cratering process [1,2]. Constraining the relative proportions of these two rim components for craters of different sizes is essential in understanding how craters grow [e.g. 1] and distribute their ejecta [e.g., 3, 4]. Relying on LRO NAC images and the best available DTMs, I have measured the maximum local heights of 299 coherent bedrock exposures around the upper walls of 21 fresh lunar craters ranging in diameter from 2.2 km to 45 km. The tops of these outcrops provide a *minimum* constraint on the amount of wallrock uplift, WU_{\min} , from which the *maximum* thickness T_{\max} of superposed ejecta, can be determined from $h - WU_{\min}$, where h is the rim height measured from the pre-impact surface.

Results: Linear regression of the 299 individual measurements of h , WU_{\min} and T_{\max} yields $WU_{\min} = 0.80h$ [$R^2=0.91$] and $T_{\max} = 0.20h$ [$R^2=0.16$]. The proportion of total rim height represented by ejecta, therefore, is 3 to 4 times less than that predicted from HE craters and small-scale impact experiments, i.e., T/h measured from lunar craters hovers consistently around 0.2 whereas T/h values reported for synthetic craters range between 0.6 and 0.8 [5-8].

Fig. 1a compares the average measured h for each of the lunar craters with the h -to- R scaling relationships of [9] (dotted line). Given that $h = WU + T$ and $T = 0.2h$ (equation 1), the scaling relationship between T and R (Fig.1b) for complex craters ($D \geq 17$ km) becomes:

$$T = 3.95(\pm 1.19)R^{0.399} \quad (1)$$

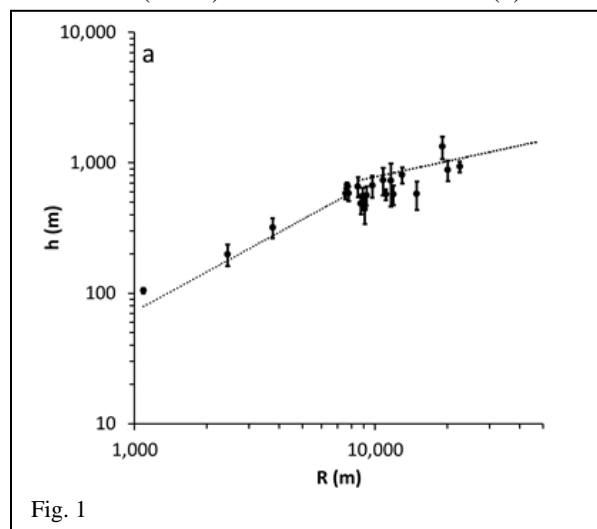


Fig. 1

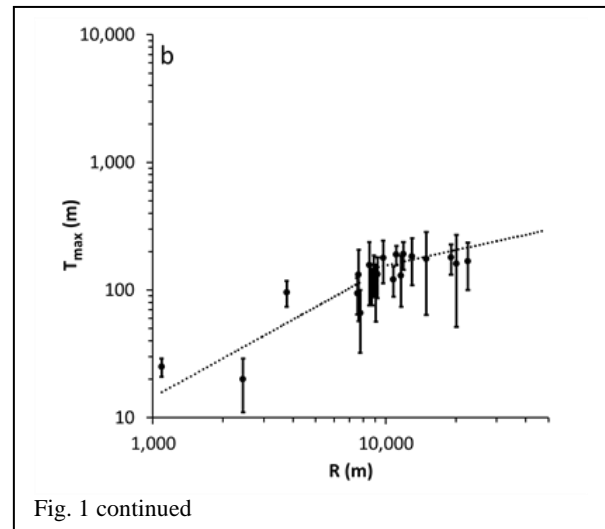


Fig. 1 continued

Discussion: The results presented above indicate that subsurface injection, rather than ballistic ejection, may be the primary mechanism of crater growth during the waning phases of the excavation stage as rim construction begins. Below, I address possible mechanisms to account for wall uplift and discuss implications concerning ejecta thickness models and excavation depth estimates.

Wall uplift mechanisms. The radially extensive structural uplift revealed by this analysis is not consistent with simple bulking or dilation of the excavation cavity wall as proposed by [2]. Bedrock exposures occur as coherent structural packages that, in several cases, exceed 3 km in length and over 500 m in thickness. Parallel to the crater wall the layers consistently appear horizontal or near-horizontal over extensive lateral distances, with only minor folding and faulting, not the jumbled, crumpled appearance that would be consistent with dilated or highly deformed wall rock. These observations are most consistent with outward, sill-like injection of impact melt and/or breccia into the target rocks surrounding the growing crater.

The interpretation that rim uplift is due to systematic near-horizontal injection into the crater wall rocks is consistent with observations at both Barringer and Lomar craters. Both craters show upper wall rocks that are systematically tilted outwardly: at Lomar 10° - 30° outward dips typify the upper wall rocks [10]. Although Barringer Crater exhibits intensified faulting at its joint-controlled 'corners', in more typical 'linear' segments of the crater walls the beds of the upper walls

show 35°-40° dips away from the crater center [11]. Neither Lonar nor Barringer craters express the chaotic block arrangements that would support the bulking hypothesis.

Ejecta thickness models. Assuming equation (1) holds for larger complex craters on the Moon, ejecta deposits on the rims of multiring basins such as Imbrium ($D=1,160$ [12]) are considerably thinner than predicted by previous models. For instance, the widely used model of [3], i.e., $T = 0.14R^{0.74}$ predicts 2,577 m of ejecta on Imbrium's rim whereas by equation (1) $T = 787$ m (± 235 m).

Equation 1 seems to predict surprisingly thin ejecta blankets compared to previous estimates based on geological assessments of landscape modification. For instance, [13] measured remnant relief on craters covered by the Orientale ejecta blanket to arrive at a maximum ejecta thickness of 2900 ± 300 m at Orientale's rim (i.e., the Cordilleran ring; $R=465$ km) whereas equation 1 predicts $T = 723 \pm 217$ m. However, the approach [13] used measures the total thickness of the basin's ejecta blanket which comprises both basin-derived ejecta and locally incorporated material due to ballistic sedimentation [14]. Material launched at high velocity along ballistic trajectories interacts violently with the local target surface, eroding relief and incorporating large amounts of local material in the final ejecta deposit. This would be the case even at the final rim ring of large basins such as Orientale, where ejecta throw distances would be hundreds of kilometers.

By focusing on relatively small impact craters, the effects of ballistic sedimentation are minimized (but not eliminated) in the data presented here because the launch trajectories of rim ejecta are relatively short (and therefore less energetic) compared to larger basin-forming events. Accepting the estimate of [13], for instance, the amount of basin-derived ejected material at the Cordillera is $\leq 25\%$ of the total deposit thickness, an estimate that is consistent with the results of [15] who constrained the proportions of basin- and locally derived ejecta based on a study of the 26-km lunar crater Deslisle.

Excavation depth. It is generally accepted [e.g., 2] that the maximum depth of excavation $d_e \cong 0.1 D_e$, the diameter of the excavation cavity. Observations presented here, however, indicate that ejecta deposits near lunar crater rims are ~ 3 - 4 times thinner than previously thought implying that the total volume of excavated material is comparably smaller. This indicates that the actual excavation cavity volume is smaller by an equivalent amount. Furthermore, if excavation volume and depth are correlated, as commonly assumed [1,2] then the maximum crater excavation depth would be

somewhat less than $1/3^{\text{rd}}$ the value of the previous estimate, i.e.:

$$d_e \leq 0.03D_e \quad (2)$$

Recent geological evidence appears to support such a shallow excavation depth: The ~ 2500 -km South Pole-Aiken (SPA) basin [16], is the largest known impact basin on the Moon. High resolution gravity data from the recent Gravity Recovery and Interior Laboratory (GRAIL) mission [17] in combination with LRO's Lunar Observer Laser Altimeter (LOLA) [18], have shown that the lunar crust is only ~ 40 km thick [19]. By $d_e \cong 0.1 D_e$, the SPA impact event should have excavated deep (i.e., $d_e \geq 125$ km) into the lunar mantle and ejected a significant quantity of material with mantle affinity. However, there are no wide-spread units with a possible mantle affinity beyond the basin floor of SPA [20-21] demonstrating that the SPA-forming event did not excavate deeply, if at all, into the lunar mantle. Using equation (2), however, the estimated maximum depth of excavation for SPA would lie between ~ 35 km and ~ 55 km. Consequently, the shallow excavation depth model proposed here is much more consistent with current geological and geophysical observational constraints on crustal composition and thickness than previous estimates.

References: [1] Croft, S. K. (1981) *Multi-ring Basins*, *PLPS 12A*, 207-225. [2] Melosh, H. J. (1989) *Impact Cratering: A Geologic Process*. [3] McGetchin T. R. et al. (1973) *EPSL 20*, 226-236. [4] Pike, R. J. (1974) *EPSL 23*, 265-274. [5] Carlson, R. H. and Jones, D. G. (1965) *JGR 70*, 1897-1910. [6] Dillon, L. A. (1972) *AFWL-TR-71-144*. [7] Stöffler D. D. et al., (1975) *JGR 80*, 4062-4077. [8] Cooper, H. F. (1977) *Impact Explos. Cratering*, 11-44. [9] Pike, R. J. (1977) *Impact Explos Cratering*, 489-509. [10] Maloof, A. C. et al., (2010) *GSA Bull. 122*, 109-126. [11] Kring, D. A. (2007) Guidebook to the geology of Barringer Meteorite Crater. [12] Spudis, P. D. (1993) Geology of Multi-ring Basins. [13] Fassett, C. I. et al. (2011) *GRL 38*, doi: 10.1029/2011GL048502. [14] Oberbeck, V. R. (1975) *Rev. Geophys. Sp. Phys.*, 337-362. [15] Morrison, R. H. and Oberbeck, V. R (1978) *PLPSC 9th*, 3763-3785. [16] Spudis, P. D. et al., (1994), *Science 266*, 1848-1851. [17] Zuber, M. T. et al., (2012) *Science 339*, 668-671. [18] Smith, D. E. et al., (2010) *Space Sci. Rev. 150*, 209-242. [19] Wiczorek, M. A. et al., (2013) *Science 339*, 671-675. [20] Lucey, P. G. (2004) *GRL 31* doi: 10.1029/2003/GL019406. [21] Wiczorek, M. A. et al., (2006), *rev. Min & Geochem.* 221-364.